Title

Effect of taxane-based neoadjuvant chemotherapy on fibroglandular tissue volume and percent breast density in the contralateral normal breast evaluated by 3T MR

Journal

NMR in Biomedicine, 26(12)

ISSN

0952-3480

Authors

Chen, Jeon-Hor

Pan, Wei-Fan

Kao, Julian

et al.

Publication Date

2013-12-01

DOI

10.1002/nbm.3006

Peer reviewed

Research article

NMR IN BIOMEDICINE

Received: 26 November 2012, Revised: 1 July 2013, Accepted: 2 July 2013, Published online in Wiley Online Library

(wileyonlinelibrary.com) DOI: 10.1002/nbm.3006

Effect of taxane-based neoadjuvant chemotherapy on fibroglandular tissue volume and percent breast density in the contralateral normal breast evaluated by 3T MR

Jeon-Hor Chen[a,b]*, Wei-Fan Pan[c], Julian Kao[a], Jocelyn Lu[a], Li-Kuang Chen[a], Chih-Chen Kuo[c], Chih-Kai Chang[c], Wen-Pin Chen[d], Christine E. McLaren[d], Shadfar Bahri[a], Rita S. Mehta[e] and Min-Ying Su[a]

The aim of this study was to evaluate the change of breast density in the normal breast of patients receiving neoadjuvant chemotherapy (NAC). Forty-four breast cancer patients were studied. MRI acquisition was performed before treatment (baseline), and 4 and 12 weeks after treatment. A computer-algorithm-based program was used to segment breast tissue and calculate breast volume (BV), fibroglandular tissue volume (FV), and percent density (PD) (the ratio of FV over BV × 100%). The reduction of FV and PD after treatment was compared with baseline using paired *t*-tests with a Bonferroni–Holm correction. The association of density reduction with age was analyzed. FV and PD after NAC showed significant decreases compared with the baseline. FV was 110.0 ml (67.2, 189.8) (geometric mean (interquartile range)) at baseline, 104.3 ml (66.6, 164.4) after 4 weeks ($p < 0.0001$), and 94.7 ml (60.2, 144.4) after 12 weeks (comparison with baseline, $p < 0.0001$; comparison with 4 weeks, $p = 0.016$). PD was 11.2% (6.4, 22.4) at baseline, 10.6% (6.6, 20.3) after 4 weeks ($p < 0.0001$), and 9.7% (6.2, 17.9) after 12 weeks (comparison with baseline, $p = 0.0001$; comparison with 4 weeks, $p = 0.018$). Younger patients tended to show a higher density reduction, but overall correlation with age was only moderate ($r = 0.28$ for FV, $p = 0.07$, and $r = 0.52$ for PD, $p = 0.0003$). Our study showed that breast density measured from MR images acquired at 3T MR can be accurately quantified using a robust computer-aided algorithm based on non-parametric non-uniformity normalization (N3) and an adaptive fuzzy C-means algorithm. Similar to doxorubicin and cyclophosphamide regimens, the taxane-based NAC regimen also caused density atrophy in the normal breast and showed reduction in FV and PD. The effect of breast density reduction was age related and duration related. Copyright © 2013 John Wiley & Sons, Ltd.

Keywords: breast density; normal breast; neoadjuvant chemotherapy; taxane; MRI; fibroglandular tissue volume; percent density; 3T MR

INTRODUCTION

Neoadjuvant chemotherapy (NAC) can induce tumor shrinkage, improve operability, and increase the rate of breast-conserving surgery (1). NAC may also potentially eradicate small breast cancer foci in the contralateral breast, but a more important risk reduction mechanism may come from ovarian suppression (2,3), namely, chemotherapy-induced amenorrhea (CIA). Observational studies have reported that chemotherapy can result in 30%–70% reduction in the risk of developing contralateral breast cancer (4–7). The benefit can last over 10 years after diagnosis (3). In a recent report by the Early Breast Cancer Trialists'

* *Correspondence to: Jeon-Hor Chen, Tu and Yuen Center for Functional Onco-Imaging, Department of Radiological Sciences, University of California Irvine, CA, USA.*
E-mail: jeonhc@uci.edu

a *J.-H. Chen, J. Kao, J. Lu, L.-K. Chen, S. Bahri, M.-Y. Su*
Tu and Yuen Center for Functional Onco-Imaging, Department of Radiological Sciences, University of California Irvine, CA, USA

b *J.-H. Chen*
Department of Radiology, E-Da Hospital and I-Shou University, Kaohsiung, Taiwan

c *W.-F. Pan, C.-C. Kuo, C.-K. Chang*
Department of Medicine, School of Medicine, China Medical University, Taichung, Taiwan

d *W.-P. Chen, C. E. McLaren*
Department of Epidemiology, University of California Irvine, CA, USA

e *R. S. Mehta*
Department of Medicine, University of California Irvine, CA, USA

Abbreviations used: *NAC, neoadjuvant chemotherapy; FV, fibroglandular tissue volume; PD, percent breast density; CMF, cyclophosphamide, methotrexate and fluorouracil; 2D, two dimensional; 3D, three dimensional; AC, doxorubicin and cyclophosphamide; IDC, invasive ductal carcinoma; ILC, invasive lobular carcinoma; ER, estrogen receptor; SENSE, sensitivity encoding; FOV, field of view; T_R, repetition time; T_E, echo time; NSA, number of signal average; N3, non-parametric non-uniformity normalization; FCM, fuzzy C-means; CCR, clinical complete response; pCR, pathological complete response; CIA, chemotherapy-induced amenorrhea; BV, breast volume; DCE-MRI, dynamic contrast-enhanced MRI.*

Collaborative Group (8) that included 194 randomized treatment trials, it was found that chemotherapy can decrease risk of developing contralateral breast cancer in women younger than 50 years, but not among women over 50 years old. However, it is difficult to provide accurate assessment of chemotherapy-related protection effects due to the lack of quantitative biomarkers.

Estrogen, which is mainly secreted by the ovary in premenopausal women, is known to be a powerful mitotic agent as well as a proliferation and growth factor inductor (9). A recent study showed that endogenous hormones were positively correlated with breast density in premenopausal women (10). The effect of chemotherapy on the histological changes of the normal breast tissue, possibly due to the reduced secretion of endogenous hormones in women with ovarian suppression, has been elaborated. These changes include reduction of the lobular acini, lobular sclerosis, and the attenuation of the lobular/ductal epithelium (11). Signs of cell proliferation are absent and there is no mitotic activity. These findings provide the pathological basis of breast density reduction following NAC. Both breast density and circulating estrogen are known as independent risk factors associated with the development of breast cancer (12). Density reduction in the contralateral breast following NAC due to ovarian suppression may therefore potentially be used as a biomarker to assess future cancer risk.

The extent of ovarian suppression due to NAC is related to a patient's age, the specific chemotherapy agents and the total administered dose (13). Among the wide variety of NAC regimens being used, alkylating agents, e.g. the combination regimen of oral CMF (cyclophosphamide, methotrexate, and fluorouracil), are associated with a high risk of ovarian failure (14). Only a few studies have investigated ovarian function in women treated with taxane-based chemotherapy (15–17).

NAC-induced density reduction can be evaluated with imaging modalities. Breast density analyzed based on two dimensional (2D) mammography suffers from the problem of overlapping tissues and does not provide a true volumetric measurement. MRI provides a three-dimensional (3D) view of the breast with strong soft tissue contrast; hence it may provide a more precise volumetric measurement with which to evaluate the change of breast density following therapy. 2D mammographic measurements of density are usually higher than those of corresponding 3D MR density values. This difference may be due to the inherent problem of overlapping tissues that affect density measurements made by 2D mammography.

Only a few studies have reported breast density measurement using MRI (12,18–26). A 3D MRI density method with high reproducibility and small measurement variation has been reported (18,19). The method therefore is useful for measurement of breast density over time. In most other studies breast segmentation was performed using preset criteria for consistency. These studies did not aim to develop a reliable method for any individual or for longitudinal measurements. A study by Eng-Wong *et al*. (20) found that, in premenopausal women at increased risk for breast cancer who were receiving raloxifene, mean mammographic density did not show statistically significant changes but mean MR breast density showed significant reduction. Based on the results it was suggested that MR breast density is more sensitive for detecting small changes, thus it may provide a promising surrogate biomarker and should be investigated further.

The reduction of breast density in MRI, acquired at 1.5T MR, in NAC patients receiving doxorubicin and cyclophosphamide (AC) followed by taxane-based regimens has been previously investigated. Significant density reduction was shown after initial treatment with one to two cycles of AC regimen (27). In that study, taxane treatment was given after AC, and further significant density reduction during taxane regimen was not observed. Because a great reduction in density had already occurred during the AC regimen, the effect of taxane on the change of breast tissue could not be evaluated.

Due to the concern of cardiac toxicity of AC, taxane-based regimens have become more widely used as the first-line NAC regimen for breast cancer. The availability of this new NAC protocol allowed us to examine the effect of taxane-based drugs on changes in breast tissue. The purpose of this study was to investigate the change of breast density at 4 weeks and 12 weeks after starting taxane-based NAC regimens by using a quantitative volumetric method applied to 3D MR images acquired by 3T MR.

MATERIALS AND METHODS

Subjects

This study was approved by the institutional review board and complied with the Health Insurance Portability and Accountability Act. Over a period of three years (June 2008 and June 2011), 55 patients with biopsy-proven breast cancer gave written informed consent to participate in the NAC treatment study and receive MRI for response monitoring. Only patients who had completed MRI studies at three times, before treatment and after 4 and 12 weeks of treatment, were included in this analysis. Eleven patients were excluded, including the following: two did not have a baseline MRI before starting chemotherapy, five had only one follow-up MRI at 4 weeks, and one had only one follow-up MRI at 12 weeks. Of the remaining 44 patients (age range 28–82; mean age 47 years, median age 48 years), 29 patients were 50 years old or less and 15 were more than 50 years old. The histologic tumor types included 37 invasive ductal carcinomas (IDCs), four invasive lobular carcinomas (ILCs), two IDCs with lobular features, and one IDC with squamous metaplasia. Sixteen of the 44 patients were Her-2−, 25 were Her-2+, and three had no report of Her-2 status. Twenty-five patients had estrogen receptor (ER) positive cancers while 19 patients had ER negative cancers. Among the 44 patients reported in this study, 30 of them had been included in a study (28). However, the design and purpose of these two studies were completely different. The purpose of the previous study was to assess how the molecular biomarker status of breast cancer, including Her-2, hormonal receptor, and the proliferation marker Ki-67, affects MR diagnosis.

Neoadjuvant chemotherapy protocol

Each patient received a taxane-based regimen, which included weekly paclitaxel and carboplatin, in combination with weekly trastuzumab for Her-2+ patients or biweekly bevacizumab for Her-2− patients.

MRI acquisition

The MRI acquired at 3T was performed on a Philips Achieva scanner (Philips Medical Systems, Best, Netherlands) with a

NMR IN BIOMEDICINE

dedicated, sensitivity encoding (SENSE)-enabled, bilateral four-channel breast coil. The precontrast non-fat-suppressed sequence was acquired with a 2D turbo spin echo with repetition time T_R = 800 ms, echo time T_E = 8.6 ms, flip angle = 90°, matrix size = 480 × 480, field of view (FOV) = 31–38 cm, and slice thickness = 2 mm. In the 3T Philips system, a setting called 'CLEAR' (Constant Level Appearance) was mandatory in all 'SENSE' enabled scans to increase the uniformity of each image.

The bilateral axial dynamic contrast-enhanced MRI (DCE-MRI) was acquired using a 3D gradient-echo, fat-suppressed sequence with FOV = 31–36 cm, acquisition slice thickness = 2 mm, reconstructed slice thickness = 1 mm, slice overlap=1 mm, image matrix 480 × 480, T_R/T_E = 6.2/1.26 ms, flip angle = 12°, number of signal average (NSA) =1, SENSE-factor = 2. Seven dynamic frames, including two pre-enhanced and five post-enhanced, were acquired. The imaging temporal resolution was 1 min 38 s for each frame. In this study only the non-contrast T_{1W} images without fat suppression were used for measurement of breast density.

MR-based breast density analysis

Breast and fibroglandular tissue segmentation was performed using a modified published method (18,19) by a research assistant (W.-F. Pan) with a background in radiological technology and medical imaging and one year of experience in segmenting breast MR images. This method has small measurement errors, with an intra-operator variation of 2.8% and an inter-operator variation of 3.8% (18). The measurement variation caused by body position is in the range of 3%–4% (18).

Before performing segmentation, the operator viewed the entire axial T_{1W} image dataset and determined the superior and inferior boundaries of the breast (the beginning and ending slices) by comparing the thickness of breast fat with that of body fat. Non-breast subcutaneous fat on the chest typically displays a homogenous thickness across the chest wall, which was used to determine the boundaries of the breast.

The breast segmentation procedures consisted of the following. (1) A coronal cut was performed to exclude the thoracic region. Depending on the morphology of the breast, a transverse line was drawn along the posterior margin of each individual subject's sternum. If some fibroglandular tissues were not included, the horizontal line was lowered, up to 35 mm posterior from the original sternum landmark. This was done to ensure that the analyzed breast region was consistent, and that the entire fibroglandular tissue was contained within the segmented breast. (2) Fuzzy-C-means (FCM) clustering and B-spline curve fitting were applied to obtain the breast–chest boundary. In this step, the operator checked each slice and determined if the pectoralis muscle had been removed adequately. If not, the operator had to modify the boundary manually. (3) A novel method based on non-parametric non-uniformity normalization (N3) and an adaptive FCM algorithm (19) was used to remove the strong intensity non-uniformity and correct the bias field for segmentation of fibroglandular tissue and fatty tissue. Bias field is an undesirable signal caused by inhomogeneities in the magnetic field. The N3 algorithm is a fully automatic histogram-based method, and is a popular correction method widely used in the literature (29). The N3 algorithm is able to reduce the bias field while avoiding the problem of generating erroneous contrast. (4) Dynamic searching was applied to exclude the skin along the breast boundary. (5) The standard FCM algorithm was applied to classify all pixels on the image. The default setting was to use a total of six clusters, three for fibroglandular tissue, and three for fatty tissues. In recent years we had applied the segmentation method to many other studies and found that using N = 6, 3 for fibroglandular and 3 for fatty tissues was the optimal setting that could achieve satisfactory results in many different types of MR image acquired using different pulse sequences and different scanners. After completing the process, the dense tissue ROI was mapped onto the original MRI and the operator went through the images slice by slice to inspect the segmentation quality by comparing the segmented images with the original non-segmented images. If the quality analyzed using this setting was not satisfactory, the operator could choose to use a different cluster number, typically by decreasing the total cluster number from six to five, with two or three clusters as the dense tissue. The reason why the segmentation worked with a given cluster size for one patient but not for another was most likely the difference of breast tissue compositions and tissue contrast subject to subject. The segmentation setting and parameters used for the baseline MRI study of a patient were used for all her follow-up MRI studies, so the calculated percent change was not affected by different settings.

To ensure accurate segmentation, the operators checked the segmented images slice by slice and compared with the original non-segmented T_{1WI}. In case of segmentation error(s), several strategies were used for the correction (30). These errors included fatty tissue mistakenly segmented as fibroglandular tissue because of incomplete bias field correction, inclusion of nipple, and incomplete segmentation of fibroglandular tissue because of partial volume effect. Strategies that were applied for error correction included the following: (a) further improvements were made in field inhomogeneity correction; (b) the breast region was resegmented by using a different landmark; (c) nipple exclusion was redone using computer algorithms; (d) the local contrast was changed; and (e) the FCM cluster setting was changed for segmentation (30). Quantitative breast volume (BV), fibroglandular tissue volume (FV), and percent density (PD, calculated as the ratio of FV over BV × 100%), were obtained. The analysis of the whole set of images for both breasts of a subject, including the corrections, could be completed in 45 min.

Statistical analysis

We applied the Shapiro–Wilk test of normality to FV and PD values measured at each time point. Because statistically significant differences from normality were observed for the distributions of values measured at baseline and at 4 and 12 weeks of treatment, the natural log transformation was applied to FV and PD values. There were no significant differences from normality for the distributions of log transformed FV values measured at baseline (p = 0.48), 4 weeks of treatment (p = 0.64), and 12 weeks of treatment (p = 0.70), nor for log transformed PD values measured at baseline (p = 0.19), 4 weeks of treatment (p = 0.42), and 12 weeks of treatment (p = 0.55).

Independent sample t-tests were applied to compare baseline mean values of the natural log of FV and PD between pre- and post-menopausal women, ER+ and ER− cancer, and Her-2+ versus Her-2− cancer. The Bonferroni–Holm method of multiple comparisons was applied to maintain an overall significance level of 0.05 for each outcome. Using the Bonferroni–Holm method, for each outcome variable k = 3 tests were performed and the unadjusted

p-values (p_i) were ordered from smallest to largest. For a significance level of 0.05, if $p_i \leq 0.05/(k - i + 1)$ then one can conclude that there is a statistically significant difference for the *i*th test. If $p_i > 0.05/(k - i + 1)$ then one can conclude that there is insufficient evidence of a statistically significant difference for the *i*th test. Paired *t*-tests were applied to examine the mean difference from baseline in transformed values of FV and PD at 4 weeks and at 12 weeks, and the mean difference in transformed values of FV and PD measured at 4 versus 12 weeks. Paired *t*-tests also were utilized to evaluate the percent reduction of FV and PD measured during (4 weeks of treatment) and after NAC (12 weeks of treatment) compared with the baseline.

Using independent sample *t*-tests, the percent reduction in FV and PD from baseline to 12 weeks was compared for ER+ versus ER− cancer, Her-2+ versus Her-2− cancer, and clinical complete response and/or pathological complete response (CCR/pCR) versus non-(CCR/pCR). The Bonferroni–Holm method of multiple comparisons was applied to maintain an overall significance level of 0.05 for each outcome. Pearson's correlation was used to investigate the association of FV and PD reduction with age.

RESULTS

Breast density before and after neoadjuvant chemotherapy

The baseline MRI was analyzed to compare FV and PD between the pre- and post-menopausal women; and between women with different biomarker statuses (Table 1). All means reported are geometric means unless otherwise noted. The FV of the pre-menopausal women (≤50, $N = 29$) was significantly higher than that of the peri- and post-menopausal women (>50, $N = 15$) (134.4 ml versus 74.7 ml, nominal $p = 0.0017$). PD was also significantly higher in pre-menopausal women than the post-menopausal women (14.7% versus 6.6%, $p = 0.0017$). ER+ cancer did not show significant differences in either FV or PD compared with ER− cancer (107.7 ml versus 113.1 ml, $p = 0.80$ for FV; 10.1% versus 12.8%, $p = 0.30$ for PD). Women with Her-2+ cancer ($N = 16$) did not show significant differences in baseline FV or PD from those for women with Her-2− breast cancer ($N = 25$) (91.3 ml versus 124.6 ml, $p = 0.12$ for FV; 10.0% versus 12.1%, $p = 0.45$ for PD).

FV and PD were measured at baseline and at two follow-up MRI studies for each patient, and the percent reduction at 4 and 12 weeks was calculated with respect to baseline values. Table 2 shows group averages for FV and PD from three MRI studies and the mean percent reduction of FV and PD calculated from follow-up MRI studies compared with the baseline. FV was 110.0 ml (67.2, 189.8) (geometric mean (interquartile range)) at baseline and 104.3 ml (66.6, 164.4) after 4 weeks (paired *t*-test, nominal $p < 0.0001$), and showed a further decrease to 94.7 ml (60.2, 144.4) after 12 weeks (paired *t*-test for comparison with baseline, nominal $p < 0.0001$; paired *t*-test for comparison with 4 weeks, nominal $p = 0.016$). PD was 11.2% (6.4, 22.4) at baseline and 10.6% (6.6, 20.3) after 4 weeks (paired *t*-test, nominal $p < 0.0001$), and showed a further decrease to 9.7% (6.2, 17.9) after 12 weeks (paired *t*-test for comparison with baseline, nominal $p = 0.0001$; paired *t*-test for comparison with 4 weeks, nominal $p = 0.018$).

The percent reduction of FV and PD was correlated with the baseline FV and PD. Moderate correlation was noted in all of the analyses (percent reduction of FV versus baseline FV, $r = 0.41$, $p = 0.006$; percent reduction of FV versus baseline PD, $r = 0.39$, $p = 0.009$; percent reduction of PD versus baseline PD, $r = 0.50$, $p = 0.0005$).

Association of density reduction with age

The age effect on the percent reduction of FV and PD after 12 weeks NAC was studied. Younger patients were more likely to show a higher density reduction. The overall correlation with age was significant for reduction of PD ($r = 0.52$, $p = 0.0003$) but not significant for reduction of FV ($r = 0.28$,

Table 1. Comparison of baseline fibroglandular tissue volume and percent breast density measured by MRI. Descriptive statistics and *p*-values for independent sample *t*-tests tests are presented

Group	*N*	Mean	Standard deviation	Median	Geometric mean (i.e. $\exp^{Mean}$)	25th pctl	75th pctl	Nominal *p*-value for independent sample *t*-test[a]
Outcome variable: $\log_e$(FV (ml) at baseline)								
Pre-menopausal women	29	4.90	0.50	4.84	134.39	4.51	5.35	*0.0017*
Post-menopausal women	15	4.31	0.64	4.09	74.68	3.89	4.71	
ER+ cancer	25	4.68	0.67	4.54	107.71	4.09	5.35	0.7983
ER− cancer	19	4.73	0.55	4.71	113.08	4.51	5.18	
Her-2+ cancer	16	4.51	0.63	4.53	91.26	4.01	4.94	0.1181
Her-2− cancer	25	4.82	0.59	4.76	124.58	4.38	5.35	
Outcome variable: $\log_e$(PD% at baseline)								
Pre-menopausal women	29	2.69	0.60	2.77	14.68	2.20	3.19	*0.0017*
Post-menopausal women	15	1.88	0.73	1.80	6.57	1.40	2.28	
ER+ cancer	25	2.31	0.84	2.27	10.07	1.63	3.11	0.2984
ER− cancer	19	2.55	0.61	2.41	12.79	1.98	3.11	
Her-2+ cancer	16	2.30	0.85	2.10	10.01	1.72	3.08	0.4482
Her-2− cancer	25	2.49	0.73	2.41	12.10	1.88	3.18	

[a]*p*-values in italic indicate statistically significant results, adjusted for multiple comparisons.

NMR IN BIOMEDICINE

Table 2. Breast density reduction at 4 weeks and 12 weeks treatment

Measure	Time	Geometric mean (interquartile range)	*p*-value for comparison with baseline*	Percent reduction from baseline (mean ± SD)
FV (ml)	Baseline	110 (67.2, 189.8)		
	4 weeks	104.3 (66.6, 164.4)	$p < 0.0001$	4.3 ± 12.7
	12 weeks	94.7 (60.2, 144.4)	$p < 0.0001$	12.2 ± 15.6
PD (%)	Baseline	11.2 (6.4, 22.4)		
	4 weeks	10.6 (6.6, 20.3)	$p < 0.0001$	4.1 ± 13.8
	12 weeks	9.7 (6.2, 17.9)	$p < 0.0001$	11.1 ± 19.1

*Paired *t*-test for comparison of mean difference in $\log_e$(FV) measured at 4 weeks versus 12 weeks ($p = 0.016$) and in $\log_e$(PD) ($p = 0.018$).

$p = 0.07$), as illustrated in Fig. 1. Figs 2–5 show examples of three pre-menopausal women with remarkable FV reduction after NAC, and one post-menopausal woman with a smaller reduction in FV.

Density reduction versus biomarker status

Overall, women harboring ER+ cancer ($N = 25$) did not show a statistically significant difference in the percent reduction of FV and PD after 12 weeks NAC compared with baseline, for measurements made in their contralateral normal breasts, compared with women with ER− cancer ($N = 19$) (mean ± SD 14.8 ± 13.3% versus 9.6 ± 17.6%, nominal $p = 0.26$ for FV; 13.1 ± 17.0% versus 9.0 ± 21.4%, nominal $p = 0.26$ for PD). The percent reduction of FV and PD after NAC also did not differ significantly between women with Her-2+ cancer and women with Her-2− breast cancer (9.7 ± 17.1% versus 14.9 ± 13.2%, $p = 0.28$ for FV; and 10.8 ± 23.9% versus 11.7 ± 16.0%, $p = 0.88$ for PD) (Table 3).

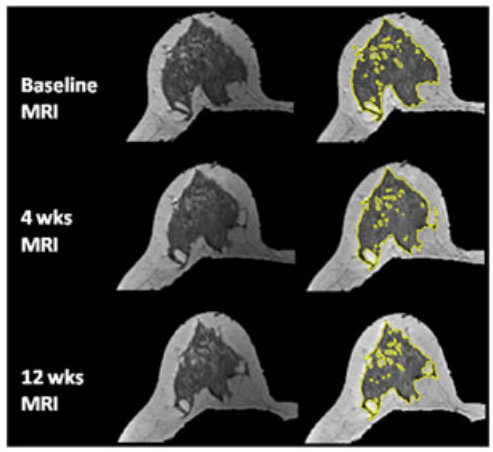

Figure 2. A 40 year-old woman with central type breast morphology. The percent reduction is 12.2% for FV and 11.9% for PD after 4 weeks treatment; and 30% for FV and 35% for PD after 12 weeks treatment.

Density reduction versus baseline tumor size and tumor response

The percent reduction of FV and PD after 12 weeks NAC treatment was correlated with the pre-treatment tumor size (range = 1.5–15 cm, mean ± SD =5.3 ± 2.8 cm) but no significant correlation was noted ($r = 0.18$, $p = 0.24$ for FV reduction and $r = 0.36$, $p = 0.02$ for PD reduction). Of the 44 patients, 16 patients (nine pre- and seven post-menopausal) achieved CCR/pCR; 28 patients (20 pre- and eight post-menopausal) were non-(CCR/pCR) (still showing remarkably enhanced residual tumor in DCE-MRI). When comparing the percent reduction of FV and PD in these two groups (CCR/pCR versus non-(CCR/pCR)), no statistically significant difference was noted (7.1 ± 15.0% versus 15.7 ± 15.0%, nominal $p = 0.07$ for the comparison of % FV reduction; 8.4 ± 22.7% versus 13.0 ± 16.6%, nominal $p = 0.44$ for the comparison of % PD reduction) (Table 3).

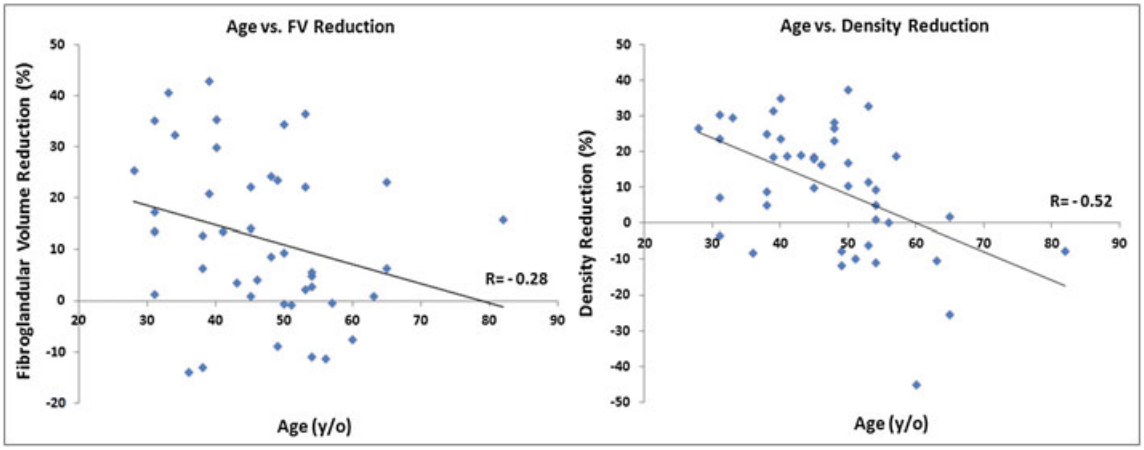

Figure 1. Correlation of decreased fibroglandular tissue volume (left) and percent density (right) with patient's age.

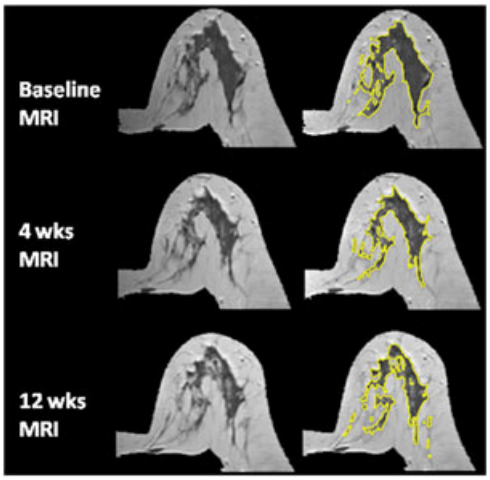

Figure 3. A 39 year-old woman with fatty breast. The percent reduction is 29.2% for FV and 27.8% for PD after 4 weeks treatment; and 43% for FV and 32% for PD after 12 weeks treatment.

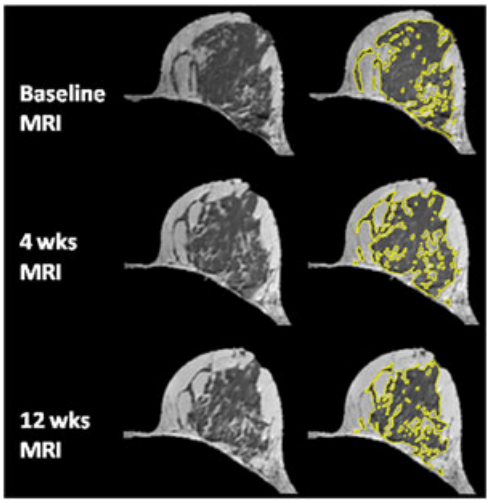

Figure 4. A 31 year-old woman with intermingled type breast morphology. The percent reduction is 13.2% for FV and 8.7% for PD after 4 weeks treatment; and 35% for FV and 30% for PD after 12 weeks treatment.

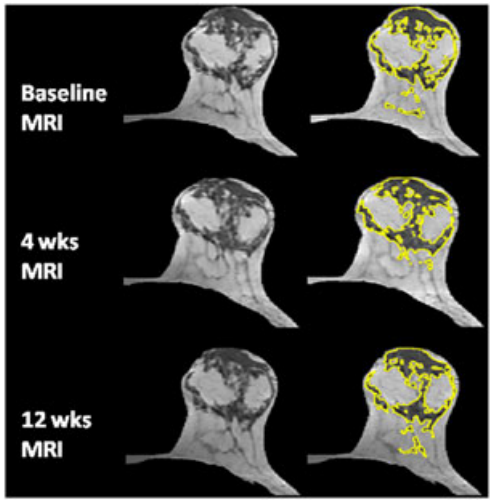

Figure 5. A 54 year-old woman with intermingled type breast morphology. The percent reduction is –3.9% for FV and 2.7% for PD after 4 weeks treatment; and 4.9% for FV and 9.4% for PD after 12 weeks treatment.

DISCUSSION

The risk of contralateral second breast cancer rates ranges from 10% to 15% at 15 years after treatment and is even higher for longer-term survivors (31,32). Factors associated with the increased risk of contralateral breast cancer are not fully understood. Lifestyle and reproductive factors (33), as well as genetic factors (34), are involved in the etiology. Breast cancer survivors are considered as high risk. In addition to regular screening and hormonal therapy (for patients with hormonal positive cancer), they may also choose prophylactic approaches to reduce risks of contralateral second breast cancer (35). A purpose of developing robust markers for predicting the risk of contralateral second breast cancer is to assist patients in choosing the most appropriate risk reduction strategies.

In this study we used 3D MR images, acquired at 3T, to evaluate the breast density reduction in the contralateral normal breast following taxane-based NAC treatment. A previous study (27) has shown that the reduction of breast density, measured from MR images acquired at 1.5T, following NAC treatment with AC can be quantified based on an FCM method. Although 3T MRI can provide images of high signal-to-noise ratio and high spatial resolution (36), the potential high field inhomogeneity may compromise the image quality (37–39), and make the segmentation of fibroglandular tissue inaccurate. With the newly developed computer-aided algorithm based on N3+FCM (19), it was, however, noted that the fibroglandular tissue segmentation could be accurately performed in most women.

Mammographic density is an independent risk factor for breast cancer, and there is also evidence suggesting that a change in density is associated with altered cancer risk (40–43). In one report it was found that an increase in BI-RADS density category within 3 years was associated with an increase in breast cancer risk; and a decrease in density associated with a decreased risk (42). Recently Cuzick *et al*. showed that, in high-risk patients receiving tamoxifen for chemoprevention, only women experiencing a 10% or greater reduction in breast density benefited from a protective effect of the therapy, with 63% reduction in breast cancer risk, whereas those showing less than a 10% reduction in breast density had no risk reduction compared with placebo (43). Based on these results, the density reduction in the normal breast of NAC patients may be used as a surrogate marker for predicting the protective effect of chemotherapy to decrease contralateral cancer risk.

Evaluation of breast density change following NAC has seldom been studied. In a previous study it was shown that patients receiving AC plus taxane NAC showed reduction of breast density. The reduction effects were already significant after initial treatment with one to two cycles of an AC regimen (27). It was also found that density reduction is associated with the ages of patients, suggesting that the effect is mediated through the suppression of ovarian function (27). Since taxane is usually given after AC in most oncological practice, the sole effect of taxane on ovarian function is difficult to assess. With our current new NAC protocol based on a taxane regimen, in this study we found that the taxane treatment also causes decreased density, but its effect is not as strong as that caused by an AC regimen. We found mean reductions of 4.3% in FV and 4.1% in PD after 4 weeks of taxane, which were less than the mean density reduction of 8.0% following one to two cycles of AC (27). The results suggest that the effect of taxane on the

Table 3. Comparison of percent reduction of fibroglandular tissue volume and percent breast density. Descriptive statistics and *p*-values for independent sample *t*-tests are presented

Group	*N*	Mean	Standard deviation	Median	25th pctl	75th pctl	Nominal *p*-value for independent sample *t*-test[a]
Outcome variable: percentage reduction in FV from baseline = (FV at week 12 − FV at baseline) × 100%/(FV at baseline)							
CCR/pCR	16	−7.08	14.97	−3.86	−18.43	4.14	0.0740
Non-(CCR/pCR)	28	−15.67	14.95	−13.82	−24.84	−4.26	
ER+ cancer	25	−14.83	13.32	−14.07	−23.63	−5.72	0.2634
ER− cancer	19	−9.55	17.63	−4.07	−22.27	0.60	
Her-2+ cancer	16	−9.68	17.13	−4.25	−25.45	0.50	0.2794
Her-2− cancer	25	−14.89	13.19	−14.07	−23.12	−6.45	
Outcome variable: percentage reduction in PD% from baseline = (PD% at week 12 − PD% at baseline) × 100%/(PD% at baseline)							
CCR/pCR	16	-8.44	22.68	−10.27	−17.87	7.55	0.4448
Non-(CCR/pCR)	28	−13.03	16.55	−18.76	−25.83	−0.63	
ER+ cancer	25	−13.12	16.98	−10.62	−23.86	−1.03	0.2634
ER− cancer	19	−9.04	21.37	−16.32	−19.04	7.71	
Her-2+ cancer	16	−10.75	23.91	−10.03	−24.26	5.15	0.8764
Her-2− cancer	25	−11.72	16.00	−16.32	−23.86	−1.03	

[a]There were no statistically significance differences between groups, adjusted for multiple comparisons.

suppression of ovarian function was not as acute as that of AC. After 12 weeks of taxane treatments, the mean reduction was 12.2% in FV and 11.1% in PD, which were comparable to the 11.3% density reduction after four cycles of AC at 8 weeks (27). Overall, although the group analysis from our study has shown reductions in FV and PD following NAC treatment, there were still some subjects who showed paradoxical findings of increased FV ($N = 9$) and increased PD ($N = 11$). Upon further examination of data from these subjects, it was noted that eight of the 11 women showed an increased PD. This was due to the decrease of breast volume after NAC compared with the baseline breast volume, which resulted in the "false increase" of PD. In longitudinal breast MRI studies, such as ours, the variation of breast positioning of the same patient time to time, although carefully handled, can always be a source of error for calculating PD. The mild increase of FV after NAC, found in nine women, might have been due to the fact that we did not control the timing of breast MRI studies. This might cause inconsistent measurement of FV during menstrual cycle.

In our study we have found that women 50 years old or less had significantly higher FV and PD than women more than 50 years old. The results were consistent with a previous study showing that FV and PD are age dependent (44). In the analysis of density reduction with age, we found a significant trend of higher reduction of PD ($r = 0.52$, $p = 0.0003$) in younger patients, which was consistent with previous findings in patients undergoing AC treatment (27). If the density reduction was from the direct damage to the breast tissue due to chemotherapy, the percent reduction should not have been dependent on age; therefore, a more plausible explanation was that the observed density reduction was due to decreased systemic hormones from the damage to the ovary, which is more pronounced in younger patients. The reduction of FV was, however, not significantly correlated with age ($r = 0.28$, $p = 0.07$).

In this study we also investigated the difference of baseline PD and density reduction following NAC between women harboring ER+ and ER− cancers. Our results were consistent with those of a previous study (45) that showed no significant differences in breast density between ER+ and ER− patients. We found that women with ER+ cancer showed more remarkable reductions of FV and PD in their contralateral breasts than women with ER− cancer. However, the observed differences were not statistically significantly different. Recent studies have shown that endogenous hormones affect density in premenopausal women, and there was a positive association between estrogen levels and breast density (10,46). The association between serum sex hormones and premenopausal breast cancer risk was inconclusive (47). The difference of endogenous hormonal level between ER+ and ER− cancer in premenopausal women has not been previously reported. Findings from a study of postmenopausal women with breast cancer, however, found that women with ER−/PR− breast cancers had lower circulating levels of all measured sex steroid hormones than women with ER+/PR+ breast cancers (48). Women of Her-2+ and Her-2− cancers, although receiving different NAC treatment combinations, one with trastuzumab and the other with bevacizumab, also did not show differences in density reduction following NAC. The results suggested that the density reduction might mainly come from the ovarian suppression effect of the taxane regimen, and may not be related to the molecular target regimens.

In this study, we also assessed the correlation between baseline tumor size and tumor response with the reduction of FV and PD in the contralateral normal breast. The growth of breast cancer demands tumor angiogenesis. Studies comparing mammary arteries supplying bilateral breasts have found that the breast harboring breast cancer showed remarkably more prominent vascular supply than the contralateral normal breast (49–51). The increase of ipsilateral breast vascularity is associated with tumor size (49,50). When receiving NAC, a larger tumor and its harboring breast may receive more chemotherapy regimens, which results in relatively less delivery of chemotherapy regimens to the contralateral normal breast. If a direct toxic effect exists, there should be an inverse correlation of baseline tumor size with reduction of FV and PD. However, the results from

our study did not provide strong evidence to support this assumption. Similarly, women with CCR/pCR presumably have more effective blood flow and chemotherapy regimen delivery into the tumor and the diseased breast, hence less reduction of FV and PD in the contralateral normal breast, than patients with non-(CCR/pCR). Our results showed that women with non-(CCR/pCR) had greater reduction of FV and PD, on average, than women with CCR/pCR, but the difference was not statistically significant.

This study had limitations. Here we only evaluated breast density change in women receiving NAC treatment. The study could be considerably strengthened by including information about cancer recurrence and breast cancer survival rate. We studied a small number of cases, prohibiting us from further analysis of the differences in mean density reduction in women with different density types. In some women with fatty breast and low breast density, it was difficult to perform accurate density segmentation, and this might have made the longitudinal evaluation of the density changes unreliable. In this study, despite the fact that the observed density reduction following NAC was small, statistical analysis has demonstrated the significance of our results. However, we acknowledge that our results may be confounded by two factors. First, the 3D MR density method had small measurement variation ($<5\%$). Second, due to various factors such as patient convenience and/or preferences, we did not schedule breast MRI according to the timing of menstrual cycles, which could affect density measurements due to the fluctuation in breast density over the menstrual cycle.

In conclusion, the results from our study showed that NAC using taxane-based regimens also had a similar effect on the reduction of FV and PD as did AC, and the effect was age related and duration related. The currently used computer-aided algorithm based on N3+FCM was able to quantify the reduction of breast density measured from MR images acquired at 3T MR. For patients with cancer in one breast, the risk of developing another cancer in the contralateral breast is increased, thus these patients are followed as a high-risk population. Since quantitative measures of FV and PD can be obtained on MRI, the reduction of these two parameters after NAC may potentially be used as imaging biomarkers to correlate with future cancer risk occurring in the contralateral normal breast.

COMPETING INTERESTS

The authors declare that they have no competing interests.

AUTHORS' CONTRIBUTIONS

J.H.C. designed the case–control study used for this analysis, carried out the literature review, interpreted the results, and drafted the manuscript. J.K., J.L., L.K.C., C.C.K., and C.K.C. collected the clinical data and MR images. W.F.P. ran the computer algorithm and did the breast and fibroglandular tissue segmentations. S. B. and R.S.M. recruited subjects and performed breast MRI studies. M.Y.S. designed the case–control study and interpreted the results. W.P.C. and C.E.M. did the statistical tests. All authors edited the manuscript and approved the final manuscript submitted for publication.

Acknowledgement

This work was supported in part by NIH/NCI grants R01 CA127927, R21 CA170955 and R03 CA136071. Statistical support for this project was provided by the Biostatistical Shared Resource of the Chao Family Comprehensive Cancer Center, University of California, Irvine, CA.

REFERENCES

1. van der Hage JA, van de Velde CJ, Julien JP, Tubiana-Hulin M, Vandervelden C, Duchateau L. Preoperative chemotherapy in primary operable breast cancer: results from the European Organization for Research and Treatment of Cancer Trial 10902. J. Clin. Oncol. 2001; 19(22): 4224–4237.
2. Warne GL, Fairley KF, Hobbs JB, Martin FI. Cyclophosphamide-induced ovarian failure. N. Engl. J. Med. 1973; 289(22): 1159–1162.
3. Bertelsen L, Bernstein L, Olsen JH, Mellemkjaer L, Haile RW, Lynch CF, Malone KE, Anton-Culver H, Christensen J, Langholz B, Thomas DC, Begg CB, Capanu M, Ejlertsen B, Stovall M, Boice JD Jr, Shore RE, Women's Environment, Cancer and Radiation Epidemiology Study Collaborative Group, Bernstein JL. Effect of systemic adjuvant treatment on risk for contralateral breast cancer in the Women's Environment, Cancer and Radiation Epidemiology Study. J. Natl. Cancer Inst. 2008; 100(1): 32–40.
4. Bernstein JL, Thompson WD, Risch N, Holford TR. Risk factors predicting the incidence of second primary breast cancer among women diagnosed with a first primary breast cancer. Am. J. Epidemiol. 1992; 136: 925–936.
5. Broët P, de la Rochefordière A, Scholl SM, Fourquet A, Mosseri V, Durand JC, Pouillart P, Asselain B. Contralateral breast cancer: annual incidence and risk parameters. J. Clin. Oncol. 1995; 13: 1578–1583.
6. Horn PL, Thompson WD. Risk of contralateral breast cancer. Associations with histologic, clinical, and therapeutic factors. Cancer 1988; 62: 412–424.
7. Schaapveld M, Visser O, Louwman WJ, Willemse PH, de Vries EG, van der Graaf WT, Otter R, Coebergh JW, van Leeuwen FE. The impact of adjuvant therapy on contralateral breast cancer risk and the prognostic significance of contralateral breast cancer: a population based study in the Netherlands. Breast Cancer Res. Treat. 2008; 110(1): 189–197.
8. The Early Breast Cancer Trialists' Collaborative Group. Effects of chemotherapy and hormonal therapy for early breast cancer on recurrence and 15-year survival: an overview of the randomised trials. Lancet 2005; 365: 1687–1717.
9. Stines J, Tristant H. The normal breast and its variations in mammography. Eur. J. Radiol. 2005; 54: 26–36.
10. Walker K, Fletcher O, Johnson N, Coupland B, McCormack VA, Folkerd E, Gibson L, Hillier SG, Holly JM, Moss S, Dowsett M, Peto J, dos Santos Silva I. Premenopausal mammographic density in relation to cyclic variations in endogenous sex hormone levels, prolactin, and insulin-like growth factors. Cancer Res.. 2009; 69(16): 6490–6499.
11. Schnitt SJ, Collins LC. *Biopsy Interpretation of the Breast Treatment Effects*. Lippincott Williams and Wilkins: Philadelphia, PA, 2009; 435–439.
12. Khazen M, Warren RM, Boggis CR, Bryant EC, Reed S, Warsi I, Pointon LJ, Kwan-Lim GE, Thompson D, Eeles R, Easton D, Evans DG, Leach MO, Collaborators in the United Kingdom Medical Research Council Magnetic Resonance Imaging in Breast Screening (MARIBS) Study. A pilot study of compositional analysis of the breast and estimation of breast mammographic density using three-dimensional T_1-weighted magnetic resonance imaging. Cancer Epidemiol. Biomarkers Prev. 2008; 17(9): 2268–2274.
13. Gadducci A, Cosio S, Genazzani AR. Ovarian function and childbearing issues in breast cancer survivors. Gynecol. Endocrinol. 2007; 23(11): 625–631.
14. Bines J, Oleske DM, Cobleigh MA. Ovarian function in premenopausal women treated with adjuvant chemotherapy for breast cancer. J. Clin. Oncol. 1996; 14(5): 1718–1729.
15. Fornier MN, Modi S, Panageas KS, Norton L, Hudis C. Incidence of chemotherapy-induced, long-term amenorrhea in patients with breast carcinoma age 40 years and younger after adjuvant anthracycline and taxane. Cancer 2005; 104: 1575–1579.

16. Davis AL, Klitus M, Mintzer DM. Chemotherapy-induced amenorrhea from adjuvant breast cancer treatment: the effect of the addition of taxanes. Clin. Breast Cancer 2005; 6: 421–424.
17. Petrek JA, Naughton MJ, Case LD, Paskett ED, Naftalis EZ, Singletary SE, Sukumvanich P. Incidence, time course, and determinants of menstrual bleeding after breast cancer treatment: a prospective study. J. Clin. Oncol. 2006; 24: 1045–1051.
18. Nie K, Chen JH, Chan S, Chau MK, Yu HJ, Bahri S, Tseng T, Nalcioglu O, Su MY. Development of a quantitative method for analysis of breast density based on three-dimensional breast MRI. Med. Phys. 2008; 35(12): 5253–5262.
19. Lin M, Chan S, Chen JH, Chang D, Nie K, Chen ST, Lin CJ, Shih TC, Nalcioglu O, Su MY. A new bias field correction method combining N3 and FCM for improved segmentation of breast density on MRI. Med. Phys. 2011; 38(1): 5–14.
20. Eng-Wong J, Orzano-Birgani J, Chow CK, Venzon D, Yao J, Galbo CE, Zujewski JA, Prindiville S. Effect of raloxifene on mammographic density and breast magnetic resonance imaging in premenopausal women at increased risk for breast cancer. Cancer Epidemiol. Biomarkers Prev. 2008; 17(7): 1696–1701.
21. Wei J, Chan HP, Helvie MA, Roubidoux MA, Sahiner B, Hadjiiski LM, Zhou C, Paquerault S, Chenevert T, Goodsitt MM. Correlation between mammographic density and volumetric fibroglandular tissue estimated on breast MR images. Med. Phys. 2004; 31(4): 923–942.
22. van Engeland S, Snoeren PR, Huisman H, Boetes C, Karssemeijer N. Volumetric breast density estimation from full-field digital mammograms. IEEE Trans. Med. Imaging 2006; 25(3): 273–282.
23. Lee NA, Rusinek H, Weinreb J, Chandra R, Toth H, Singer C, Newstead G. Fatty and fibroglandular tissue volumes in the breasts of women 20–83 years old: comparison of X-ray mammography and computer-assisted MR imaging. Am. J. Roentgenol. 1997; 168: 501–506.
24. Yao J, Zujewski JA, Orzano J, Prindiville S, Chow C. Classification and calculation of breast fibroglandular tissue volume on SPGR fat suppressed MRI. SPIE Proc. 2005; 5747: 1942–1949.
25. Klifa C, Carballido-Gamio J, Wilmes L, Laprie A, Lobo C, Demicco E, Watkins M, Shepherd J, Gibbs J, Hylton N. Quantification of breast tissue index from MR data using fuzzy cluster. Proc. IEEE Eng. Med. Biol. Soc. 2004; 3: 1667–1670.
26. Thompson DJ, Leach MO, Kwan-Lim G, Gayther SA, Ramus SJ, Warsi I, Lennard F, Khazen M, Bryant E, Reed S, Boggis CR, Evans DG, Eeles RA, Easton DF, Warren RM, UK study of MRI screening for breast cancer in women at high risk (MARIBS). Assessing the usefulness of a novel MRI-based breast density estimation algorithm in a cohort of women at high genetic risk of breast cancer: the UK MARIBS study. Breast Cancer Res. 2009; 11(6): R80.
27. Chen JH, Nie K, Bahri S, Hsu CC, Hsu FT, Shih HN, Lin M, Nalcioglu O, Su MY. Decrease in breast density in the contralateral normal breast of patients receiving neoadjuvant chemotherapy: MR imaging evaluation. Radiology 2010; 255(1): 44–52.
28. Chen JH, Bahri S, Mehta RS, Kuzucan A, Yu HJ, Carpenter PM, Feig SA, Lin M, Hsiang DJ, Lane KT, Butler JA, Nalcioglu O, Su MY. Breast cancer: evaluation of response to neoadjuvant chemotherapy with 3.0-T MR imaging. Radiology 2011; 261(3): 735–743.
29. Sled JG, Zijdenbos AP, Evans AC. A nonparametric method for automatic correction of intensity nonuniformity in MRI data. IEEE Trans. Med. Imaging 1998; 17: 87–97.
30. Chan SW, Su MY, Lei FJ, Wu JP, Lin MQ, Nalcioglu O, Stephen F, Chen JH. Menstrual cycle related fluctuations in breast density measured by 3D MRI. Radiology 2011; 261(3): 744–751.
31. Freedman GM, Anderson PR, Hanlon AL, Eisenberg DF, Nicolaou N. Pattern of local recurrence after conservative surgery and whole-breast irradiation. Int. J. Radiat. Oncol. Biol. Phys. 2005; 61(5): 1328–1336.
32. Gao X, Fisher SG, Emami B. Risk of second primary cancer in the contralateral breast in women treated for early-stage breast cancer: a population-based study. Int. J. Radiat. Oncol. Biol. Phys. 2003; 56(4): 1038–1045.
33. Madigan MP, Ziegler RG, Benichou J, Byrne C, Hoover RN. Proportion of breast cancer cases in the United States explained by well-established risk factors. J. Natl. Cancer Inst. 1995; 87(22): 1681–1685.
34. Pharoah PD, Antoniou A, Bobrow M, Zimmern RL, Easton DF, Ponder BA. Polygenic susceptibility to breast cancer and implications for prevention. Nat. Genet. 2002; 31(1): 33–36.
35. Brenner DJ. Contralateral second breast cancers: prediction and prevention. J. Natl. Cancer Inst. 2010; 102: 444–445.
36. Rakow-Penner R, Daniel B, Yu H, Sawyer-Glover A, Glover GH. Relaxation times of breast tissue at 1.5T and 3T measured using IDEAL. J. Magn. Reson. Imaging 2006; 23: 87–91.
37. Kuhl CK, Kooijman H, Gieseke HJ, Schild HH. Effect of B_1 inhomogeneity on breast MR imaging at 3.0 T. Radiology 2007; 244: 929–930.
38. Mann RM, Kuhl CK, Kinkel K, Boetes C. Breast MRI: guidelines from the European Society of Breast Imaging. Eur. Radiol. 2008; 18: 1307–1318.
39. Azlan CA, Giovanni PD, Ahearn TS, Semple SK, Gilbert FJ, Redpath TW. B_1 transmission-field inhomogeneity and enhancement ratio errors in dynamic contrast-enhanced MRI (DCE-MRI) of the breast at 3T. J. Magn. Reson. Imaging 2010; 31: 234–239.
40. Vachon CM, Pankratz VS, Scott CG, Maloney SD, Ghosh K, Brandt KR, Milanese T, Carston MJ, Sellers TA. Longitudinal trends in mammographic percent density and breast cancer risk. Cancer Epidemiol. Biomarkers Prev. 2007; 16(5): 921–928.
41. Maskarinec G, Pagano I, Lurie G, Kolonel LN. A longitudinal investigation of mammographic density: the multiethnic cohort. Cancer Epidemiol. Biomarkers Prev. 2006; 15(4): 732–739.
42. Kerlikowske K, Ichikawa L, Miglioretti DL, Buist DS, Vacek PM, Smith-Bindman R, Yankaskas B, Carney PA, Ballard-Barbash R, National Institutes of Health Breast Cancer Surveillance Consortium. Longitudinal measurement of clinical mammographic breast density to improve estimation of breast cancer risk. J. Natl Cancer Inst. 2007; 99(5): 386–395.
43. Cuzick J, Warwick J, Pinney E, Duffy SW, Cawthorn S, Howell A, Forbes JF, Warren RM. Tamoxifen-induced reduction in mammographic density and breast cancer risk reduction: a nested case–control study. J. Natl. Cancer Inst. 2011; 103(9): 744–752.
44. Nie K, Su MY, Chau MK, Chan S, Nguyen H, Tseng T, Huang Y, McLaren CE, Nalcioglu O, Chen JH. Age- and race-dependence of the fibroglandular breast density analyzed on 3D MRI. Med. Phys. 2010; 37(6): 2770–2776.
45. Chen JH, Hsu FT, Shih HN, Hsu CC, Chang D, Nie K, Nalcioglu O, Su MY. Does breast density show difference in patients with estrogen receptor-positive and estrogen receptor-negative breast cancer measured on MRI? Ann. Oncol. 2009; 20(8): 1447–1449.
46. Yong M, Atkinson C, Newton KM, Aiello Bowles EJ, Stanczyk FZ, Westerlind KC, Holt VL, Schwartz SM, Leisenring WM, Lampe JW. Associations between endogenous sex hormone levels and mammographic and bone densities in premenopausal women. Cancer Causes Control 2009; 20(7): 1039–1053.
47. Sturgeon SR, Potischman N, Malone KE, Dorgan JF, Daling J, Schairer C, Brinton LA. Serum levels of sex hormones and breast cancer risk in premenopausal women: a case–control study (USA). Cancer Causes Control 2004; 15: 45–53.
48. Falk RT, Gentzschein E, Stanczyk FZ, Garcia-Closas M, Figueroa JD, Ioffe OB, Lissowska J, Brinton LA, Sherman ME. Sex steroid hormone levels in breast adipose tissue and serum in postmenopausal women. Breast Cancer Res. Treat. 2012; 131(1): 287–294.
49. Kul S, Cansu A, Alhan E, Dinc H, Reis A, Çan G. Contrast-enhanced MR angiography of the breast: evaluation of ipsilateral increased vascularity and adjacent vessel sign in the characterization of breast lesions. Am. J. Roentgenol. 2010; 195(5): 1250–1254.
50. Sardanelli F, Fausto A, Menicagli L, Esseridou A. Breast vascular mapping obtained with contrast-enhanced MR imaging: implications for cancer diagnosis, treatment, and risk stratification. Eur. Radiol. 2007; (Suppl. 6): F48–51.
51. Mahfouz AE, Sherif H, Saad A, Taupitz M, Filimonow S, Kivelitz D, Hamm B. Gadolinium-enhanced MR angiography of the breast: is breast cancer associated with ipsilateral higher vascularity? Eur. Radiol. 2001; 11(6): 965–969.

